



SUBJECT: MGT – Trip Report – Geophysical Assistance

25 November 2014

TO: Joyce Swartzendruber
State Conservationist, NRCS
Bozeman, MT

File Code: 330-20-7

Purpose:

The growth, control, and reclamation of saline seeps are major concerns of management in the Northern Great Plains. Field studies were conducted to evaluate the use of different electromagnetic induction (EMI) meters for the identification and characterization of saline seeps and recharge areas in north-central Montana.

Participants:

Meredith Albers, Soil Scientist, USDA-NRCS, Great Falls, MT
Kelli Coleman, Soil Conservation Technician, USDA-NRCS, Conrad, MT
Jim Doolittle, Research Soil Scientist, USDA-NRCS-NSSC, Newtown Square, PA
Michael Garverich, Geologist, USDA-NRCS, Bozeman, MT
ReNae Grantier, Office Assistant, USDA-NRCS, Bozeman, MT
Ernie Haglund, Soil Conservationist, USDA-NRCS, Shelby, MT
Patrick Hensleigh, Agronomist, USDA-NRCS, Bozeman, MT
Holly Taylor, Soil Conservationist, USDA-NRCS, Fort Benton, MT
Joyce Trevithich, Agronomist, USDA-NRCS, Great Falls, MT

Activities:

Field activities were conducted during the period of 20 to 23 October 2014.

Summary:

1. In this study, national, state and local NRCS staffs collaborated in efforts to provide improved technical soil services in support of conservation planning and program delivery in Montana. Field training and investigations using electromagnetic induction (EMI) were carried out to improve and strengthen NRCS's field assistance and conservation planning programs that involve the assessment and reclamation of saline seeps.
2. Electromagnetic induction can provide a rapid, indirect method for comprehensive, quantitative measurements of recharge and discharge areas. The use of EMI is most beneficial as a rapid reconnaissance tool to map and characterize sites and to provide preliminary indications of sampling sites that are suitable for more exhaustive coring investigations and observations.
3. As in all geophysical investigations, results from this study are interpretive and should be verified by ground-truth observations. However, the use of geophysical methods should reduce the number of these observations, direct their placement, and supplement the information gathered at these sparse and widely-spaced sampling points.

4. At sites located in Cascade and Teton Counties, the use of different EMI meters and an *EMI index* provided: semi-quantitate measure of the effectiveness of reclamation methods associated with Conservation Reserve Program (CRP), clues as to the location and magnitude of a potential seep areas, and insight into the underlying soil and stratigraphic structures.
5. The dynamic nature of soil hydrologic processes and variations in soil structures make the study of recharge and discharge areas challenging. As shown in this report, the use of EMI can provide added insight into these processes and structures.
6. An Archer-1 handheld field computer is used by Montana NRCS staffs to record and georeferenced the data from EMI meters. In this study, when used with the EM31 meter, recording problems were observed in the software used in the Archer-1. For effective and accurate measurements of field data with the EM31 meter, the recording software program needs to be further modified or a commercially available program purchased.

It was the pleasure of Jim Doolittle and the National Soil Survey Center to work in Montana and to be of assistance to you and your staff.

JONATHAN W. HEMPEL
Director
National Soil Survey Center

Attachment (Technical Report)

cc:

Meredith Albers, Soil Scientist, USDA-NRCS, Great Falls, MT
James Doolittle, Research Soil Scientist, USDA-NRCS-NSSC, Soil Survey Research & Laboratory,
Newtown Square, PA
William Drummond, State Soil Scientist, USDA-NRCS, Bozeman, MT
Moustafa Elrashidi, Research Soil Scientist/Liaison MO4, USDA-NRCS-NSSC, Soil Survey Research
& Laboratory, MS 41, Lincoln, NE
Charles Gordon, Soil Survey Regional Director, USDA-NRCS, Bozeman, MT
Luis Hernandez, Acting Director, Soil Science Division, USDA-NRCS, Washington, DC
Patrick Hensleigh, State Agronomist, USDA-NRCS, Bozeman, MT
Joyce Trevithick, Area Agronomist, USDA-NRCS, Great Falls MT
Wes Tuttle, Soil Scientist (Geophysical), USDA-NRCS-NSSC, Soil Survey Research & Laboratory,
Wilkesboro, NC
Douglas Wysocki, National Leader, Soil Survey Research & Laboratory Staff, USDA-NRCS-NSSC,
MS 41, Lincoln, NE

Technical Report

James A. Doolittle

Background:

Saline seeps are areas of groundwater discharge in dryland farming regions. In the Northern Great Plains, saline seeps are responsible for the removal of valuable agricultural land from production, deterioration of surface and shallow groundwater resources, and financial losses to farmers and ranchers (Taylor, 2013). A combination of factors helps to distinguish saline seeps from other saline areas. These factors include their recent origin, saturated root zone, shallow water table, and sensitivity to climatic variation and land management practices (Brown *et al.*, 1983). Saline seeps develop when excess water that is not absorbed by plants moves downwards through soil profiles and resurfaces in lower-lying slope positions enriched with salts dissolved from within the substrata. In this process, the downward flow of excess moisture is redirected by relatively impermeable layers within the substrata, which cause the water to perch, flow laterally, and seep to the soil surface on downslope positions, where it evaporates and leaves the salts behind as a white crust.

Seep development is related to the geology and climate of the region as well as the current crop-fallow farming system (Doering and Sandoval, 1976; Halvorson, 1988). In the northern Great Plains, dryland soil salinity (saline-seep) problems became widespread during the 1960's and 1970's (Halvorson, 1984) and were associated with the extensive use of alternate crop-fallow (summer-fallow) farming systems and periods of increased precipitation. The use of crop-fallow farming rotations reduces the amount of soil moisture used by plants, increases the deep percolation of excess water, and contributes to rising water tables and the development of saline seeps in many areas (Taylor, 2013). Once developed, saline seeps grow at an average rate of about 10% a year (Miller *et al.* 1981).

Methods are needed to determine the extent of saline seeps, track their development, and quantify the extent and speed of prescribed reclamation. A major problem in managing and reclaiming saline seeps is the identification and delineation of recharge and discharge areas so that effective management options can be applied. Presently, the identification of saline seeps is largely by direct visual observations and generally remains qualitative and subjective rather than scientific (Mankin and Karthikeyan, 2002).

Seeps are related to surficial and bedrock geology (Miller *et al.*, 1981), and generally develop on hillsides, particularly where there is a change in slope (Halvorson and Rhoades, 1974). Early indications of developing saline seep include localized high yields, wet or inaccessible fields, increasing infestations of salt tolerant weeds, sloughed hillsides, and stunted or dying trees in windbreaks or shelterbelts (Taylor, 2013). As the seep develops, salts accumulate as a white crust on the soil surface, yields are seriously reduced, and salt tolerant species become dominant (Taylor, 2013).

Electromagnetic induction (EMI) has been used to distinguish saline-seep from non-seep areas, evaluate saline seep extent, and create field-scale soil salinity maps (Williams, 1983; Williams and Arunin, 1990; Hatton, *et al.*, 1994; Richardson and Williams, 1994; Mankin and Karthikeyan, 2002; Williams *et al.*, 2006). The apparent conductivity (EC_a) measured with an EMI sensor is principally affected by variations in the soluble salt, clay, and water contents of soils (McNeill, 1980). However, in areas of saline soils, variations in soluble salt content is the principal factor affecting EC_a (William *et al.*, 2006). Williams (1983) estimated that in saline soils, 70 % of the variation in EC_a can be explained by differences in the concentration of soluble salts alone.

This study principally addresses the use of EMI in Conservation Reserve Program (CRP) areas where saline seeps have been previously recognized and deep rooted species planted to ameliorate the saline conditions.

EMI Index:

It has been said that all segments of a soil-landscape contribute to groundwater recharge unless they are actively discharging. Also, individual sites may alternate between periods of downward leaching (recharge) and upward leaching (discharge) cycles depending on different time-based circumstances. Under dominantly upward leaching and evaporative processes, salts will tend to concentrate near the soil surface in groundwater discharge sites (seeps) (Richardson and Williams, 1994). Typically, the higher concentration of soluble salts in surface layers will result in high EC_a values and inverted salt profiles (EC_a is highest in surface layers and decreases with increasing depth). In general, discharge areas will have higher EC_a values than recharge areas. Conversely, groundwater recharge sites are characterized by the downward leaching and concentration of salts at greater soil depths. As a consequence, EC_a is generally low in surface layers and increases with increasing depth (regular salt profile). In recharge areas, low soluble salt and water contents are associated with low EC_a (Mankin and Karthikeyan, 2002).

Williams and Arunin (1990) noted that EC_a measurements using multi-frequency soundings or multiple dipole orientations can be used to determine whether salt concentrations increase or decrease with increasing soil depth. These researchers observed that areas where EC_a values either increased or decreased with increasing DOI showed a high degree of correspondence with recharge and discharge areas, respectively. Williams and Arunin (1990) attempted to quantify the change in EC_a with depth by using an *EM slope*; an average ratio of deep to shallow soundings. Richardson and Williams (1995) later used an empirical *discharge index* (DI) to characterize vertical EC_a patterns. The DI is determined by dividing the shallower by the deeper EC_a measurement and multiplying this ratio by the average EC_a measurement. Mankin and Karthikeyan (2002) modified the *EMI discharge index* of Richardson and Williams (1995) and used an *EMI index* (the ratio of EM38-horizontal to EM38-vertical readings) to track the progress of saline seep remediation treatments. These researchers found the *EMI index* to be an appropriate tool for tracking relative changes in seep size and the progress of saline seep remediation treatments. The use of the *EMI index* assumes uniform soil and regolith profiles and is more open to misinterpretations where soils and regolith are variable and layered.

In this study, we calculated the *EMI index* as the ratio of the EC_a for a shallow and deep layer based on the data from two intercoil spacings or dipole orientations. In addition, this ratio was not scaled by an average magnitude as done by Richardson and Williams (1995).

Equipment:

The EM38-MK2 and EM31 meters were used in this study. These meters are manufactured by Geonics Limited (Mississauga, Ontario).¹ These meters are portable and require only one person to operate. No ground contact is required with either meter. The EM38-MK2 meter weighs about 5.4 kg (11.9 lbs.) and operates at a frequency of 14,500 Hz. When placed on the ground surface, this meter has effective depths of observation (DOI) of about 0 to 0.75 and 0 to 1.5 m in the horizontal (HDO) and vertical dipole (VDO) orientations, respectively (Geonics Limited, 2009).

The EM31 meter weighs about 12.4 kg (27.3 lbs.), has a 3.66 m intercoil spacing, and operates at a frequency of 9,810 Hz. When placed on the soil surface, the EM31 meter has effective depths of observation of about 0 to 3 and 0 to 6 meters in the HDO and VDO, respectively (McNeill, 1980). McNeill (1980) described the principles of operation for the EM31 meter. In order to collect continuous EC_a data in both dipole orientations, two separate surveys are required with the EM31 meter, each with the meter positioned in different dipole orientations. This process doubles the time required to conduct a survey.

¹ Trade names are used to provide specific information. Their mention does not constitute endorsement by USDA-NRCS.

A Pathfinder ProXT GPS receiver (Trimble, Sunnyvale, CA) was used to geo-reference the EMI data collected with the EM38-MK2 meter.² Position data were recorded at a rate of one reading per second. The Geonics DAS70 Data Acquisition System was used with the EM38-MK2 meter to record and store both EC_a and GPS data. The acquisition system consists of the EMI meter, GPS receiver, and an Allegro CX field computer (Juniper Systems, Logan, Utah).² The RTmap38-MK2 software program developed by Geomar Software Inc. (Mississauga, Ontario) was used with the EM38-MK2 meter and the Allegro CX handheld field computer to record, store, and process EC_a and GPS data.¹

An Archer-1 handheld field computer (Juniper Systems, Logan, Utah) with an internal Hemisphere XF101 DGPS receiver was used to record and geo-reference data measured with the EM31 meter.² The Archer-1 contains the Microsoft Windows Mobile 6.1 operating system, and data are recorded using the ESRI ArcGIS ARCPAD 10 program, which was encoded by staff at the Bozeman NRCS State Office.²

To help summarize the results of the EMI surveys, SURFER for Windows (version 10.0), developed by Golden Software, Inc. (Golden, CO), was used to construct the simulations shown in this report.² Grids of EC_a data were created using kriging methods with an octant search.

Survey Procedures:

The EMI meters were pulled behind John Deere Gator utility vehicles on jet sleds at speeds of about 3 to 5 m/hr.² Both meters were operated with their long axis orientated parallel with the direction of travel. The EM38-MK2 meter was operated in the VDO; the EM31 meter was operated in both the HDO and VDO. Separate surveys were required for the EM31 meter positioned in different dipole orientations. Data were recorded at a rate of two measurements per second. Where possible, soils were systematically surveyed in a back and forth manner across each site. The recorded EC_a data were not corrected to a standard temperature of 75° F.



Figure 1. On-the-go surveys were conducted using mobile platforms consisting of John Deere Gators utility vehicle pulling either the EM38-MK2 or EM31 meters in a sled.

Archer-1 Data recording:

The Montana NRCS Staff uses an Archer-1 handheld field computer. The Archer-1 has the Microsoft Windows Mobile 6.1 operating system installed, and data are recorded using the ESRI ArcGIS ARCPAD 10 program, which was encoded by the staff at the Bozeman State Office.² This program functions well with the EM38 meter owned by the USDA-NRCS State Office. However, problems were noticed with this setup when used with the EM31 meter. Noticeable time delays (about 5 to 7 seconds) were observed

² Trade names are used to provide specific information. Their mention does not constitute endorsement by USDA-NRCS.

between the reception of the GPS and EC_a data. Furthermore, time-consuming adjustments were required later during data processing to make the GPS and EC_a readings match. In addition, many of the recorded EC_a values appeared to be off by one decimal point (e.g., a reading of 301 mS/m instead of 30.1mS/m) and had to be manually adjusted during post processing.

When the Archer-1 handheld field computer was used with the EM31 meter, anomalous spikes in the recorded EC_a measurements were also observed. This was especially true for measurements obtained in the HDO. Typically, spikes were recorded as isolated, extremely high positive EC_a values. While noticeable in both dipole orientations, these spikes were more common in the measurements made with the EM31 meter operated in the HDO. These spikes were so prevalent in the raw HDO data, that the actual track of the mobile EMI survey platform across fields could be visualized in plots of the EC_a data (see upper plot in Figure 2). When the EM31 meter was later operated with the Allegro field computer and either of the commercially available RTmap31 or the Trackmaker31 software programs (developed by Geomar Software Inc., Mississauga, Ontario), these spikes were not observed.³

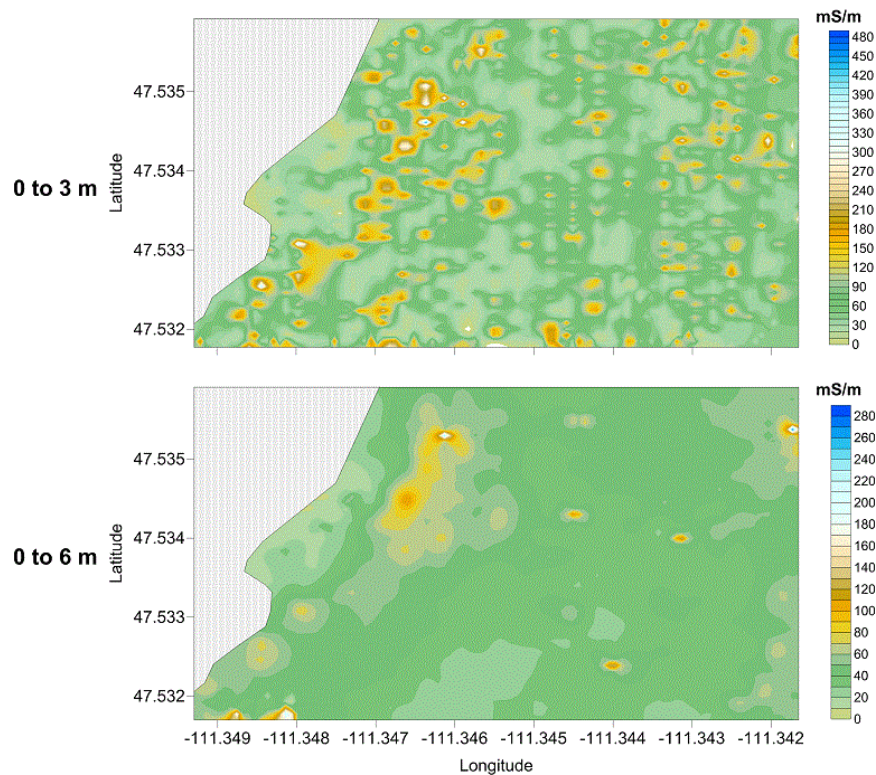


Figure 2. These two-dimensional simulations show the spatial EC_a data that were collected with the EM31 meter and an Archer handheld field computer across the lower field at the Chamberlain site. The upper and lower plots show the spatial EC_a patterns recorded in the HDO and VDO, respectively. Noticeable high amplitude spikes though most prevalent in data recorded in the HDO, are evident in both datasets.

In this study, EC_a values recorded with the EM31 meter in the HDO that were greater than 100 mS/m were considered exceptionally high and anomalous for the fields that were surveyed. Rather arbitrarily, these values were removed from the data sets recorded with the EM31 meter in the Chamberlain fields. Data recorded with the EM31 meter operated in the HDO at the Grossman site used the Allegro field computer and these spikes were not observed.

³ Trade names are used to provide specific information. Their mention does not constitute endorsement by USDA-NRCS.

Study Sites:

Miller *et al.* (1981) noted that the occurrence of saline seep is closely related to the surficial and bedrock geology. North-central Montana is underlain by predominantly dark, salt-enriched, marine shale of Cretaceous age. The *Colorado Shale* is the dominant unit underlying the study sites in both Cascade and Teton Counties. This bedrock unit is laden with salts and forms an impermeable layer, restricting the downward flow of moisture (Miller *et al.* 1981).

It is often difficult to predict the locations of saline seeps from surface topography alone, as the dip of the impermeable layer determines the direction and force of groundwater (Halvorson and Rhoades, 1974). In north-central Montana, the regional dip of the underlying sedimentary rocks is generally to the north-east at about 0.5 to 3 degrees (Miller *et al.*, 1981). The shale is easily eroded, and numerous valleys have been cut into it, with many of these valleys later filled with glacial drift (Miller *et al.*, 1981). Glacial Lake Great Falls, a large proglacial lake, once covered the area and extended from near Holter Lake to Cut Bank, Montana. At Great Falls, this lake reached depths of 600 feet (Wikipedia) and deposited the stratified sequences of sediments that now cover the area.



Figure 3. This soil map of the lower Chamberlain site is from the Web Soil Survey.

The Chamberlain study sites are located about 3.8 miles northwest of the center of Great Falls, Montana. This site consists of a lower and upper site. Both sites came out of CRP last year (2013) and portions have been used for hay this year. Both sites were under a salinity CRP contract. Figure 3 is a soil map of the lower Chamberlain site from the Web Soil Survey. The site is about 52 acres in size. The stream channel shown on this map is out-of-place, as it is located to the east of the study area. About 63 % of this site is mapped as Ethridge-Kobar silty clay loams, 2 to 8 % slopes (68). About 19 % of the site is mapped as Tally loam, 2 to 8 % slopes (189). About 11 % of this site is mapped as Assiniboine fine sandy loam, 4 to 8 % slopes (16). Also mapped within this site is a small (3.2 acres) delineation of Dooley sandy loam, 8 to 15 % slopes (55) on the western portion of this site. The very deep, well drained Assiniboine, Dooley, and Ethridge soils formed in reworked glacial lake deposits (Glacial Lake Great Falls) and/or alluvium on lower-lying stream terraces. Kobar (fine, montmorillonitic Borollic Camborthid) is an inactive soil series. The Dooley soils have 20 to 40 inches of alluvium or eolian

materials overlying the lacustrine deposits. The very deep, well drained Tally soils formed in material derived from eolian deposits, alluvium, or glaciofluvial sediments on alluvial fans and hills. The taxonomic classifications of these soils are listed in Table 1.

Table 1. Soil taxonomic classifications of the soils identified within the study sites.

| Soil Series | TAXONOMIC CLASS |
|--------------------|---|
| Arbor | Fine, smectitic, frigid Leptic Udic Haplusterts |
| Assinniboine | Fine-loamy, mixed, superactive, frigid Aridic Argiustolls |
| Cabbart | Loamy, mixed, superactive, calcareous, frigid, shallow Aridic Ustorthents |
| Dooley | Fine-loamy, mixed, superactive, frigid Typic Argiustolls |
| Ethridge | Fine, smectitic, frigid Torrertic Argiustolls |
| Evanston | Fine-loamy, mixed, superactive, frigid Aridic Argiustolls |
| Kevin | Fine-loamy, mixed, superactive, frigid Aridic Argiustolls |
| Rentsac | Loamy-skeletal, mixed, superactive, frigid Lithic Calcicustepts |
| Marvan | Fine, smectitic, frigid Sodic Haplusterts |
| Megonot | Fine, smectitic, frigid Torrertic Haplustepts |
| Pylon | Fine, smectitic, frigid Torrertic Haplustalfs |
| Scobey | Fine, smectitic, frigid Aridic Argiustolls |
| Tally | Coarse-loamy, mixed, superactive, frigid Typic Haplustolls |
| Tanna | Fine, smectitic, frigid Aridic Argiustolls |
| Yawdim | Clayey, smectitic, calcareous, frigid, shallow Aridic Ustorthents |

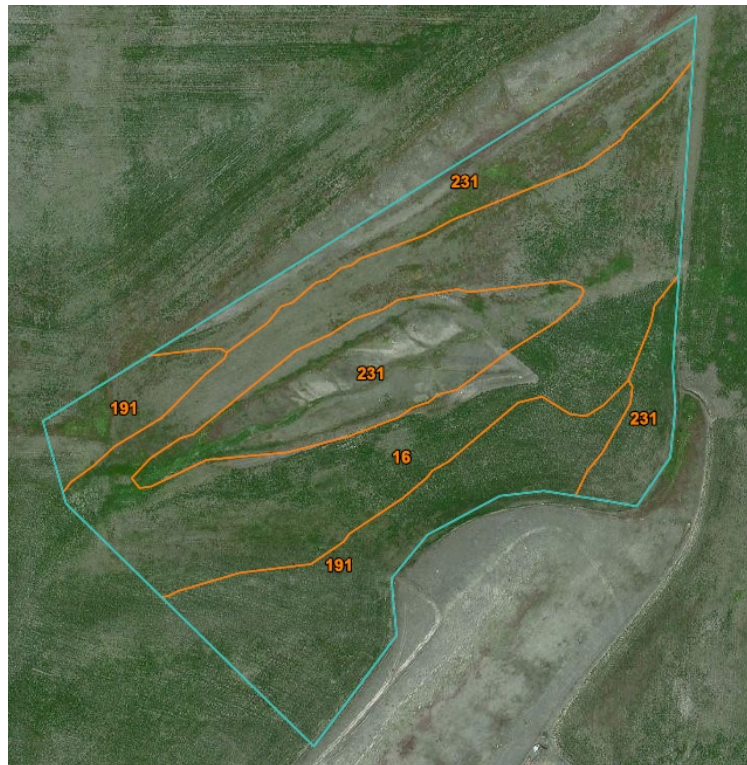


Figure 4. This soil map of the upper Chamberlain site is from the Web Soil Survey.

Figure 4 is a soil map of the upper Chamberlain site from the Web Soil Survey. The site consists of about 34 acres of hay land and CRP. About 44 % of this site is mapped as Assinniboine fine sandy loam, 4 to 8 % slopes (16). About 31 % of the site is mapped as Yawdim-Rentsac-Cabbart complex, 15 to 50 percent

slopes (231). About 24 % of the site is mapped as Tanna clay loam, 0 to 2 percent slopes (191). The more steeply sloping portions of this site are composed of Cabbart, Rentsac, and Yawdim soils. These shallow, well drained soils formed in colluvium or residuum weathered from Cretaceous-age calcareous siltstone, sandstone, and shale. The taxonomic classifications of these soils are listed in Table 1.

The Grossman site is located in Teton County. Figure 5 is a soil map of the Grossman site from the Web Soil Survey. This site is about 248 acres in size and has been in CRP for nearly 20 years. This site has highly diverse soils that vary in depth to a paralithic contact (from moderately deep to very deep), and have variable clay (mostly fine with some medium textured units) and soluble salt (non-saline and both saline and sodic soils) contents. About 62 % of the site is mapped as Pylon silty clay loam, 0 to 4 % slopes (80B). The moderately deep, well drained Pylon soils formed in residuum weathered from interbedded shale and sandstone on sedimentary uplands. Pylon soils are moderately deep (20 to 40 inches) to a paralithic contact. About 18 % of the site is mapped as Megonot-Tanna clay loams, 2 to 8 % slopes (270C). The moderately deep, well drained Megonot and Tanna soils formed in glaciofluvial deposits over semi-consolidated shale, mudstone, or siltstone. These soils are moderately deep to a paralithic contact. Compared with Tanna soils, Megonot soils lack an argillic horizon. About 10 % of the site is mapped as Scobey-Kevin clay loams, 0 to 4 % slopes (164B). The very deep, well drained Scobey and Kevin soils formed in till. Compared with Scobey soils, Kevin soils contain less clay. About 9 % of this site is mapped as Marvan silty clay, wet, 0 to 4 % slopes (540B). This delineation is mostly composed of poorly drained soils along a drainageway. The very deep, well drained Marvan soils formed in alluvium weathered from semi-consolidated shale, mudstone, or siltstone. Marvan soils have clayey subsoils with SAR ranging from 4 to 13; and EC ranging from 4 to 8 mS/cm. Also mapped within this site are very small areas (about 1.2 acres) of Abor-Yawdim silty clay loams, 2 to 8 % slopes (170C) and Megonot silty clay loam, 0 to 4 % slopes (70B). The moderately deep, well drained Abor soils formed in colluvium derived from semi-consolidated shale that is interbedded with siltstone or thin layers of sandstone. The taxonomic classifications of these soils are listed in Table 1.



Figure 5. This soil map of the Grossman site in Teton County is from the Web Soil Survey.

Results:

Chamberlain - Lower Site:

At this site, salinity is recognized and described for soil map units 68 (Ethridge-Kobar silty clay loams, 2 to 8 percent slopes) and 69 (Evanston loam, 2 to 4 percent slopes). However, for these map units, the

level of salinity ranges from only non-saline to very slightly saline (0 to 4 mmhos/cm). No mention of salinity is made in the descriptions for map units 189 (Tally loam, 2 to 8 percent slopes) and 55 (Dooley sandy loam, 8 to 15 percent slopes).

Table 2. Basic Statistics for the EC_a data collected across the lower Chamberlain field.

| | EM38-50 cm | EM38-100 cm | EM31-HDO | EM31-VDO |
|------------------|------------|-------------|----------|----------|
| Number | 7359 | 7359 | 3695 | 4874 |
| Minimum | 0.0 | 5.9 | 2.1 | 12.1 |
| 25%-tile | 9.7 | 26.7 | 22.0 | 35.3 |
| 75%-tile | 13.8 | 33.6 | 31.0 | 47.9 |
| Maximum | 44.5 | 71.2 | 93.0 | 116.4 |
| Average | 12.1 | 30.7 | 27.4 | 42.6 |
| Std. Dev. | 3.8 | 6.4 | 8.3 | 11.3 |

Basic statistics for the EC_a data collected across the lower Chamberlain site are listed in Table 2. The columns of Table 2 are arranged from left to right in order of increasing depth of observation. A majority of the measurements recorded with the EM31 meter that were above 100 mS/m and occurred as random spikes were considered erroneous and were removed from the data set. In general, EC_a increases and becomes more variable with increasing depth of observation. This trend is associated with increased moisture and the presence of finer-textured, and perhaps more salt-laden, glaciolacustrine or alluvial deposits with depth. An exception to this trend is the slightly higher average EC_a for measurements recorded with the 100-cm intercoil spacing of the EM38-MK2 meter (DOI of 0 to 1.5 m) and the slightly lower average EC_a recorded with the EM31 meter operated in the HDO (DOI of 0 to 3 m). This may be the result of errors in calibration, differences in the number and placement of measurements, and/or the prevalence of more conductivity layers between depths of about 75 to 150 cm across the survey area. As saline seeps are known to occur in this field, areas of higher conductivity are intuitively associated with higher levels of salinity.

Figure 6 contains four plots of the EC_a data that were collected across the lower Chamberlain field with the EM38-MK2 and EM31 meters. The plots are arranged from top to bottom according to increasing depths of observation. The two upper plots show spatial EC_a data measured with the 50-cm (DOI: 0 to 75 cm) and 100-cm (DOI: 0 to 150 cm) intercoil spacings of the EM38-MK2 meter. The two lower plots show spatial EC_a data measured with the EM31 meter in the HDO (DOI: 0 to 300 cm) and VDO (DOI: 0 to 600 cm). To facilitate comparison, the same color scale and color ramp have been used in each plot. The soil boundary lines shown in these plots were imported from the Web Soil Survey.

As in all geophysical investigations, results are interpretive and should be verified by ground-truth observations. The use of geophysical methods reduces the number of these observations, directs their placement, and supplements the information gathered at sparse and widely-spaced sampling points. At this site, a minimum number of soil sampling points were selected for direct observation and sampling based on the *Response Surface Sampling Design* (RSSD) program of the *ESAP* (EC_e Sampling, Assessment, and Prediction) software (Lesch, 2005; Lesch *et al.*, 2000). The RSSD program statistically selects a small number of sample locations based on the observed magnitudes and spatial distribution of the EC_a data. Based on the EC_a measurements, 6 optimal sampling points were identified in this field. However, because of mechanical problems with the probe truck, only one sample site (1S) could be cored. The location of this sampling point is shown in the plots of Figure 6.

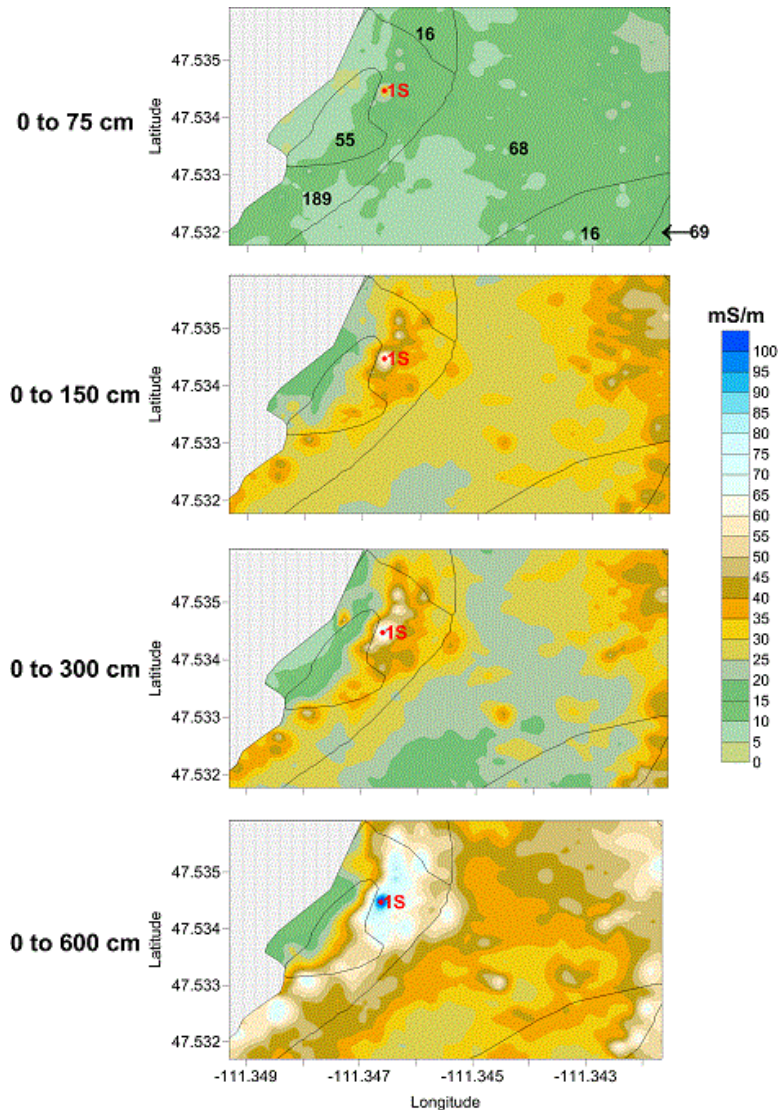


Figure 6. These two-dimensional plots of EC_a were collected with different meters, dipole orientations and intercoil spacings across the lower Chamberlain field. Apparent conductivity varies spatial within and among the different profiling depths.

As evident in the plots shown in Figure 6, EC_a increases with increasing soil depth at most locations within this site. An exception to this trend can be noted in the extreme northwestern portion of the site. With the exception of several small, isolated areas of higher EC_a located within the Tally loam on 2 to 8 % slopes map unit (189), the surface layers (0 to 75 cm) have comparatively low EC_a . These layers average only about 12 mS/m with a range of about 0 to 44 mS/m. However, within the lower portion of the 0 to 150 cm depth interval, EC_a increases across the entire site and averages about 31 mS/m with a range of about 27 to 71 mS/m. These values suggest the presence of more conductive layers present within the lower part of soil profiles. However, when deeper depths are profiled with the EM31 meter, more resistive materials are evident across the central portion of the field. For the 0 to 300 cm depth interval, EC_a becomes spatially more variable than it is within the shallower depth intervals. For the 0 to 300 cm DOI, EC_a averages about 27 mS/m with a range of about 2 to 93 mS/m. For this depth interval (0 to 300 cm), a band of more conductive materials is evident along the more sloping areas of Assinniboine, Dooley, and Talley soils in the western portion of the site. This band is associated with a relatively shallow, impervious layer that has produced a discharge area. Another band of higher EC_a is evident in

the eastern portion of the site and is associated with groundwater flow and discharge beneath Ethridge and Evanston soils from a nearby stream. With increasing DOI (0 to 600 cm), layers of more conductive materials appear to encroach upon the interior of this site from two sides (the west and east). To the west, the higher-lying area of greater EC_a is associated with a discharge area that expands along a slope break into the interior of the field. On the east, an ever broadening zone of higher EC_a encroaches into the interior of this field. Here, the increase in EC_a with increasing DOI is attributed to deeper layers of salt-enriched materials, and/or the presence of a water table with relatively high concentrations of soluble salts. The extreme northwestern portion of the field has lower EC_a which may represent thicker layers of more resistive bedrock.

In this field, only one of the six selected RSSD sampling points was cored and sampled. Sample point *IS* (see Figure 6) characterizes an area that has consistently higher EC_a at each DOI. Coring at site *IS* revealed a layer of salt accumulation at depths of 2 to 3 feet, and a high clay content layer (with lower hydraulic conductivity) around 5 feet that continued down to about 23 feet. Coring confirmed the EMI interpretation; the high EC_a at this sampling point can be associated with these physico-chemical features. It is likely that the salts accumulated along flow paths above the impervious clay layer, which is perhaps enriched with salts. As evident, in the plots shown in Figure 6, sampling point *IS* is located on a curvilinear belt of higher EC_a that is barely perceptible in the surface layers, but becomes wider and more pronounced with increasing soil depth. This belt appears to expand outwards from near point *IS* in mostly a down slope (towards east and southeast) direction. In the lower plot of Figure 6 (which shows the spatial EC_a patterns over the deepest DOI), this zone of higher conductivity achieves its greatest expression and breath, and may replicate the expanse of a salt-affected subsurface area. If saline seeps formerly occupied this site, the absence of high EC_a values near the surface (see upper plot) suggest that the deep rooted grasses and legumes planted for CRP have effectively lowered the water table and helped to ameliorate these layers of soluble salts.

The different coil orientations, coil spacings, and frequencies of the EMI sensors used in this study provide different depth responses and have helped us to visualize the location and extent of a discharge area within this site. To better understand the relationship between saline seeps and the soil-landscape, plots of EC_a data for different DOI were overlain on a three-dimensional (3D) wireframe representation of an elevation grid file from this site (see Figure 7). The elevation data were obtained during the EMI survey with the Pathfinder ProXT GPS receiver. The soil boundary lines shown in the plots of Figure 7 were imported from the Web Soil Survey. Map unit symbols for these delineations are shown in the upper left plot. The location of the lone sampling point is shown on each plot. As shown in these plots, the suspected discharge area and saline seep is largely confined to lower back slopes in the western portion of the site. The slope shape is largely concave, convex. The plots shown in Figure 7 provide additional insight into the relationship of the saline seep with the soil-landscape.

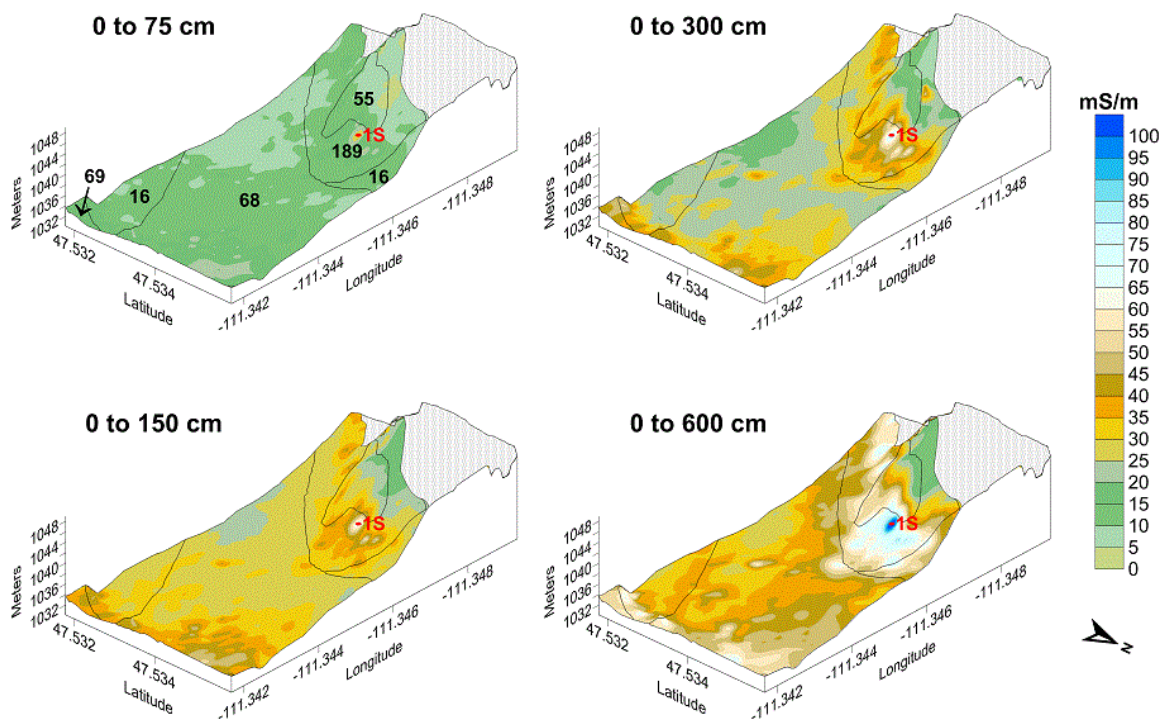


Figure 7. These three-dimensional wireframe images of the elevation at the lower Chamberlain site are overlaid by EC_a isoline plots for different depths of observation.

Figure 8 shows plots of *EMI indices* for three DOI: 0 to 150, 0 to 300, and 0 to 600 cm. Data for these plots were derived by dividing the shallower by the deeper measurements of the EM38-MK2 meter; the 100 cm intercoil spacing of the EM38-MK2 by the EM31-HDO measurements; and the EM31-HDO by the EM31-VDO measurements, respectively. In each of these plots, an *EMI index* greater than 1.0 indicated an inverted salt profile (i.e., shallow soil more saline than deeper soil). An *EMI index* less than 1.0 indicated a normal salt profile (i.e., deeper soil more saline than shallower soil).

With the exception of the 0 to 300 cm depth interval, the *EMI index* values (Figure 8) are largely distributed between 1.0 and 0.5. These values indicate that conductivity increases with depth (normal salt profiles). The contrary is seen in the plot for the 0 to 300 cm depth interval. Here the index value is greater than 1 and conductivity decreases with depth. These values suggest the presences of a more conductive layer in the lower part of the profile scanned with the EM38-MK2 meter (0 to 150 cm).

For *EMI indices* calculated with measurements from the EM38-MK2 meter (upper plot, Figure 8), the upper 150 cm of this field is characterized as a recharge area with EC_a increasing with increasing soil depth. The *EMI index* for this DOI ranges from 0.14 to 0.54. As this field was under a salinity CRP contract and had been planted to deep-root plant species, the effectiveness of these plants in reducing excess water and reducing salts in surface layers is manifested in these *EMI index* values and this plot. The *EMI indices* for the data measured with the 100 cm intercoil spacing of the EM38-MK2 meter and the EM31 meter operated in the HDO (middle plot, Figure 8) are mostly greater than 1. For these intermediate depths, most of the field is characterized by the *EMI index* as having inverted salt profile. Only small, fragmented areas in the higher-lying western portion of the field have *EMI indices* less than 1 (normal salt profile). These areas have been outlined in the western portion of the field. As sample point 1S is located within the area having an *EMI index* less than 1, the normal salt profile is attributed to the

high clay content (and perhaps salt enriched) layer observed at 5 feet. The *EMI indices* for the deepest DOI (0 to 600 cm) suggest that almost the entire field has a normal profile with EC_a increasing with increased soil depth. This trend suggests the presence of more conductive layers at greater soil depths.

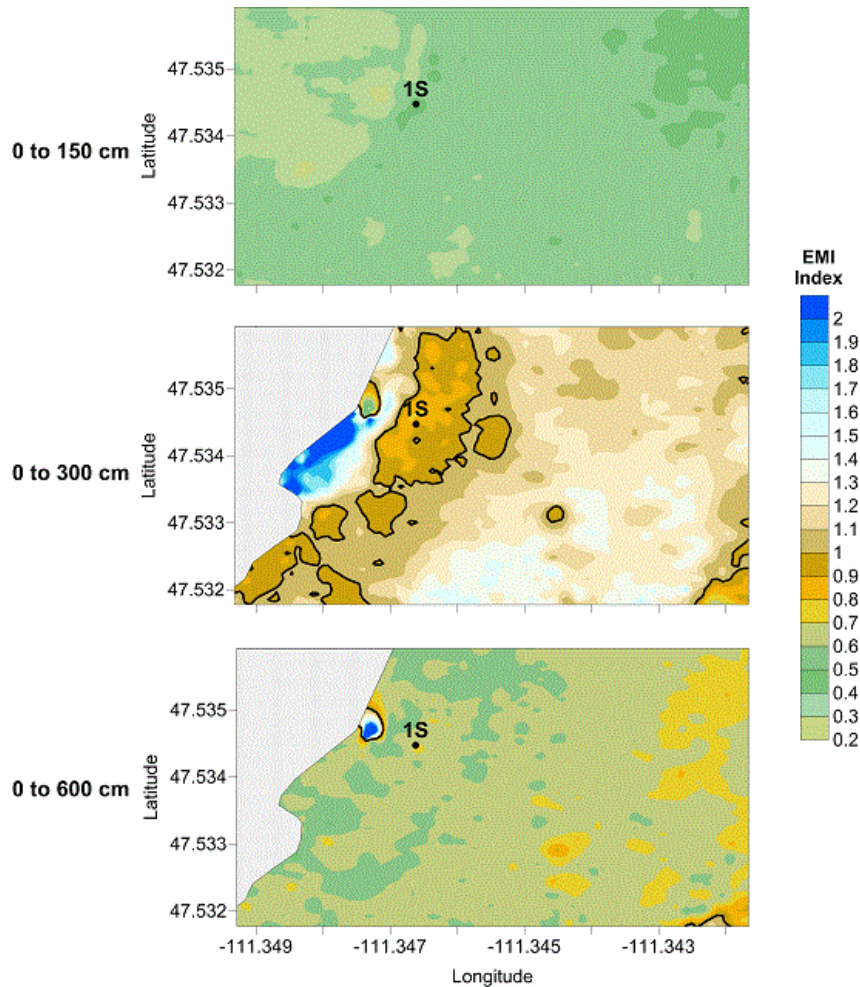


Figure 8. These two-dimensional plots of the lower Chamberlain field show the spatial distribution of EMI indices for different depths of observation.

Hatton et al. (1994) cautioned that the use of the *EMI index* is too restrictive to make this approach reliable for the identification of discharge areas in the absence of considerable knowledge of soil, hydrological and landscape factors. However, in this example, the use of multi-frequency soundings or multiple dipole orientations and *EMI indices* provided semi-quantitate measures of the effectiveness of reclamation methods associated with CRP, clues as to the location and magnitude of a potential seep area, and insight into the stratigraphic structure of this site.

Chamberlain - Upper Site:

Operation difficulties continued to be experienced using the software on the Archer field computer with the EM31 meter and numerous, anomalous and spurious responses were recorded in the upper Chamberlain fields especially when this meter was operated in the HDO. The data sets were rather subjectively edited to remove many of these seemingly anomalous and spurious responses. In addition, a pipeline passes diagonally across this field producing elevated responses. Some of these EC_a measurements were deleted from the data sets to improve the clarity of the EC_a response stemming from soil conditions. The data sets were edited and then used for statistical and image processing.

At this site, salinity is recognized and described in soil map units 231(Yawdim-Rentsac-Cabbart complex, 15 to 50 percent slopes) and 191 (Tanna clay loam, 0 to 2 percent slopes). For Yawdim-Rentsac-Cabbart complex, 15 to 50 percent slopes, salinity is described as ranging from non-saline to very slightly saline (0 to 4 mmhos/cm) for Cabbart soils, and non-saline to slightly saline (0 to 8 mmhos/cm) for Rentsac soils. On the less sloping areas of Tanna clay loam, 0 to 2 percent slopes, salinity is described as ranging from non-saline to very slightly saline (0 to 3 mmhos/cm). While no saturated paste measurement or other measure of soil salinity was available from this site, areas with relatively moderate to high levels of salinity are assumed to be present in these fields. The fields had been placed in CRP in order to improve soil quality and productivity on saline cropland by planting and maintaining a perennial plant cover.

Table 2. Basic Statistics for the EC_a data collected across the upper Chamberlain site.

| | EM38-50 cm | EM38-100 cm | EM31-HDO | EM31-VDO |
|------------------|------------|-------------|----------|----------|
| Number | 6682 | 6682 | 3171 | 3842 |
| Minimum | -1.9 | -17.3 | 3.4 | 3.4 |
| 25%-tile | 17.3 | 4.9 | 10.1 | 15.0 |
| 75%-tile | 38.2 | 24.1 | 40.7 | 60.9 |
| Maximum | 108.4 | 100.8 | 204.8 | 176.7 |
| Average | 29.1 | 12.4 | 27.4 | 39.6 |
| Std. Dev. | 15.5 | 9.4 | 20.5 | 29.1 |

Basic statistics for the EC_a data collected across the upper Chamberlain fields are listed in Table 2. The columns in Table 2 are arranged from left to right in order of increasing depth of observation. As evident in this table, the general trend is for EC_a to increase and becomes more variable with increasing DOI. The exception to this trend is the slightly lower average and less variable EC_a recorded with the 100-cm intercoil spacing of the EM38-MK2 meter (DOI of 0 to 1.5 m). This is associated with the presence of less conductivity layers between depths of about 75 to 150 cm across most of this survey area. Portions of this site are believed to be underlain by a more electrically resistive sandstone cap. Compared with the results from the lower Chamberlain field, the upper Chamberlain site has higher and less variable EC_a in the near surface layers (0 to 75 cm; EM38-50 cm), but lower and less variable EC_a in the near subsurface layers (0 to 150 cm; EM38-100cm). Also, EC_a was more variable across the upper Chamberlain field for measurements collected in with the deeper-sensing EM31 meter in both dipole orientations are similar at both sites.

Figure 9 contains four 2D plots of the EC_a data collected across the upper Chamberlain fields with the EM38-MK2 and EM31 meters. The two plots on the left show spatial EC_a data measured for DOI's of 0 to 75 cm (upper plot) and 0 to 150 cm (lower plot) with the EM38-MK2 meter. The two plots show on the right show spatial EC_a data measured for DOI's of 0 to 300 cm (upper plot) and 0 to 600 cm (lower plot) with the EM31 meter. To facilitate comparison, the same color scale and color ramp have been used in each plot. The locations and identities of four soil sampling points that were selected using the RSSD program of the ESAP software are shown on these plots. Soil boundary lines were imported from the Web Soil Survey. A subsurface pipeline bisects and trends in an east to west direction across this site. On each of the plots shown in Figure 9, a segmented, red-color line approximates the location of this buried feature. The pipeline and several other metallic artifacts scattered across this site did interfere with the EMI surveys and produced anomalous measurements, which were not completely removed from the data sets.

As evident in the plots shown in Figure 9, EC_a generally increases with increasing soil depth at most locations. In addition, EC_a increases more markedly in the northern portion of the survey area. Here two, southwest to northeast trending lines of higher EC_a appear to intersect and merge in the western portion of

the site. These lines are presumed to reflect the presence of more conductive layers associated with discharge processes.

Ground-truth cores were taken at the four points labeled in Figure 9. At 6W, cores revealed sandy materials to depths of about 18 to 19 feet, then underlying layers of cohesive clays or claystones. There were no visible salts observed in the cored from 6W. Sites 7W and 8W were also sandy, but the coring depths were restricted to 10 feet because of core refusal. Contact with sandstone was made at a depth of 1 foot below site 9S. The upper Chamberlain site is located directly above the lower Chamberlain site. Cores at the upper Chamberlain site reveal coarser textured soil materials and regolith, the occurrence of sandstone, and the absence of observable salt concentrations. These factors help to explain the lower EC_a observed across the southern portion of this site (see Figure 9) and provides clues as to the underlying structure. However, the two coalescing linear features in the northern portion of the site, were penetrated by only one soil core (7W) and the factors causing their higher EC_a may not have been observed or occurred below the restrict depth of coring (10 ft). It is presumed that the higher conductivity is associated with higher concentrations of soluble salts and excess soil moisture associated with discharge areas.

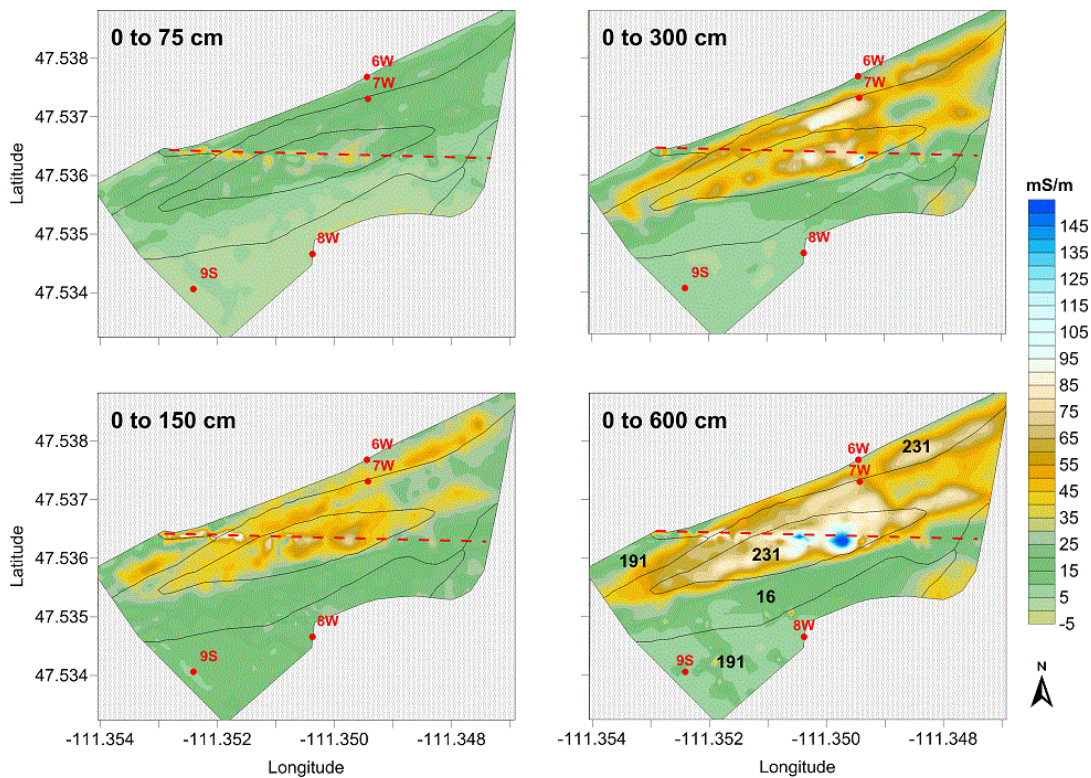


Figure 9. These two-dimensional plots of EC_a were collected with different meters, dipole orientations and intercoil spacings across the upper fields at the Chamberlain site. Variations in amplitude and spatial patterns are evident for each depth of observation.

Figure 10 contains four, 3D wireframe models of the upper fields at the Chamberlain site with draped plots of the EC_a data measured with the EM38-MK2 and EM31 meters using different intercoil spacing and/or dipole orientations. Elevation data for the 3D wireframe model were obtained during the EMI survey with the Pathfinder ProXT GPS receiver. Soil boundary lines shown in these plots were imported from the Web Soil Survey. Associated map unit symbols are shown in the upper left-hand plot. The locations of the four sampling points are shown on three of these plots (in red). As shown in these plots, areas of high EC_a (suspected saline seep) are largely confined to the swale bottom and lower backslope

positions of south-facing slopes. These are believed to be discharge areas. The higher-lying lineation of greater EC_a is believed to correspond to an outcropping of relatively impervious bedrock along which seepage is likely to occur. As there are no similar patterns on the south-facing slopes, it is assumed that the impervious layer, if present, dips downwards into the slope carrying any excess moisture away from the surface and acting as a recharge area.

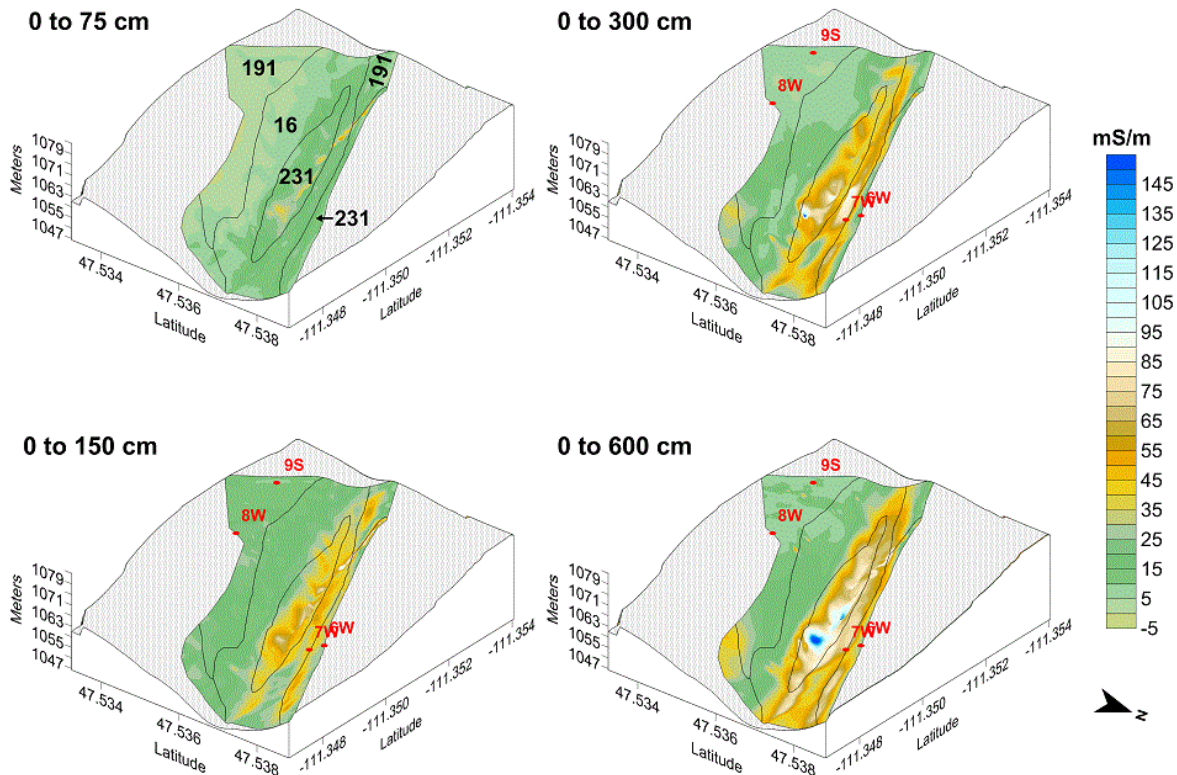


Figure 10. A three-dimensional wireframe model of the elevation at the upper Chamberlain site is overlaid by four different EC_a isoline plots; each having a different depth of observation.

The EC_a data collected over the upper fields at the Chamberlain site with the EM31 meter contained a large number of anomalous spikes. These spikes were removed from the data sets resulting in a reduced number of measurements. In addition, errors were noted in the placement of the decimal point in the recorded data resulting in need to make manual corrections to the data set. A portion of the survey area is underlain and results were affected by a buried utility line. Because of these factors it was not considered prudent or feasible to produce *EMI index* maps for the upper fields at the Chamberlain site.

At the upper Chamberlain site, the use of two different meters provided a DOI of 0 to 6 m. Using the data recorded with these two meters, spatial variations in EC_a were not only charted laterally, but over successive depth intervals. Plots revealed a zone of higher EC_a largely confined to a lower-lying swale and south facing slopes. Beneath these landscape components, EC_a increased with increasing soil depth indicating the presence of deeper increasingly more conductive layers. Soils within the southern portion of this site had relatively low EC_a . In addition as these values remained relatively uniform and did not increase noticeably with depth, the underlying layers are assumed to fairly homogenous. Considering these factors, over the DOI profiled at this site, the southern portion of the upper Chamberlain site appears to represent a recharge area.

Grossman Site:

A portion of the survey area was recently disked and exceedingly difficult to traverse with the mobile EMI platforms (see Figure 11). Portions of this site were recently disc and extremely rough to traverse. Survey speeds were significantly slowed across these fields. As a consequence, two complete surveys with the EM31 meter (each conducted in different dipole orientations) were not possible. While a survey was completed across the entire study area with the EM31 meter operated in the VDO, only the eastern portion of the survey area was surveyed with the EM31 meter operated in the HDO. As experienced at other sites, the data collected with the EM31 meter contained numerous anomalously EC_a measurements that were considered invalid. A large proportion of these measurements were removed from the data sets prior to an evaluation of the site.

At the Grossman site, salinity is recognized and described in two soil map units: Marvan silty clay, wet, 0 to 4 percent slopes (540B) and Scobey-Kevin clay loams, 0 to 4 percent slopes (164B). These soils cover about 19 % of the site. For the Marvan unit, salinity levels are described as ranging from slightly saline to moderately saline (8 to 16 mmhos/cm). In addition, Marvan soils have horizons with SAR that ranges from 4 to 38. Salinity ranges from non-saline to slightly saline (0 to 8 mmhos/cm) in areas of Scobey and Kevin soils. For the other soil map units, salinity levels are described as ranging from non-saline to very slightly saline (0 to 4 mmhos/cm). While no saturated paste measurement or other measure of soil salinity was available from this site, relatively high levels of salinity are assumed to be present in these fields. The fields had been placed in CRP in an attempt to improve soil quality and plant productivity on saline croplands by planting and maintaining a perennial plant cover over the contract period.



Figure 11. Two mobile EMI platforms survey the Grossman site in Teton County. A portion of the site had been recently disked creating a very rough surface that slowed survey speeds and reduced the number of traverses.

Basic statistics for the EC_a data collected across the Grossman fields are listed in Table 3. The columns in Table 3 are arranged from left to right in order of increasing depth of observation. The number of readings measured with the different meters and dipole orientations differed significantly. Negative values in the data set are presumed to reflect the presence of buried metallic artifacts. A buried 16-inch, steel, gas pipeline as well as buried military communication cables are known to cross these fields. The pipeline was reported to be buried at depths ranging from about 4 to 6 feet.

Table 3. Basic Statistics for the EC_a data collected across the Grossman fields.

| | EM38-50 cm | EM38-100 cm | EM31-HDO | EM31-VDO |
|------------------|------------|-------------|----------|----------|
| Number | 30686 | 30686 | 11165 | 12280 |
| Minimum | -40.9 | 11.5 | 17.1 | -54.9 |
| 25%-tile | 2.3 | 20.3 | 28.4 | 37.4 |
| 75%-tile | 10.4 | 33.8 | 43.4 | 64.8 |
| Maximum | 132.6 | 171.3 | 138.9 | 903.8 |
| Average | 10.7 | 32.9 | 38.3 | 56.2 |
| Std. Dev. | 17.1 | 23.4 | 15.6 | 33.8 |

As evident in Table 3, for each meter, EC_a increased and became more variable with increasing DOI. Because of high levels of soil salinity, these fields were placed in CRP about 18 years ago. The lower averaged EC_a in the shallower measurements (both EM38-MK2 and EM31 meters) may, in part, reflect the overall leaching of soluble salts from the upper part of soil profiles. The vertical trends measured with both meters suggest normal salt profiles in which the concentration of soluble salts and EC_a increase with increasing soil depth. However, another possible explanation is that this vertical trend reflects the presence of layers with higher moisture and clay contents at lower soil depths. Ground-truth cores are needed to verify these interpretations.

Figure 12 contains four 2D plots of the EC_a data collected across the Grossman site with the EM38-MK2 and EM31 meters. These plots are arranged from top to bottom in order of increasing depth of observation. As evident by the smaller plot in Figure 12, a reduced area was surveyed with the EM31 meter operated in the HDO (0 to 300 cm DOI). To facilitate comparison, the same color scale and color ramp have been used in each plot. The soil boundary lines were imported from the Web Soil Survey. Soil map unit symbols for these delineations are shown in the “0 to 75 cm” and the “0 to 300 cm” plots. Two subsurface utility lines are known to cut across the site, but are not clearly evident on these plots.

On the plots shown in Figure 12, patterns of consistently higher EC_a occur in the delineation of Marvan silty clay, wet, 0 to 4 percent slopes (540B). This delineation conforms to a lower-lying drainageway. The soils of this unit are saline and sodic. With increasing soil depth, EC_a increases and a well-expressed and -defined zone of higher EC_a expands outwards along the drainageway and into the nearby fields. It is assumed that excess water flows into this intermittent drainageway from adjoining slopes and over the ground surface, and temporarily ponds. Gradually, the water drains away or infiltrates into the soil and excess salts accumulate.

Also, on the plots shown in Figure 12, on the higher-lying and more sloping eastern portion of the site, several persistent, discontinuous bands of higher EC_a are evident. These bands become larger, more prominent and numerous with increasing DOI. The bands of higher EC_a are believed to mark the locations of discharge areas. Ground-truth coring should be conducted in some of these delineations to verify the presence of salts and/or excess moisture, and to confirm interpretations.

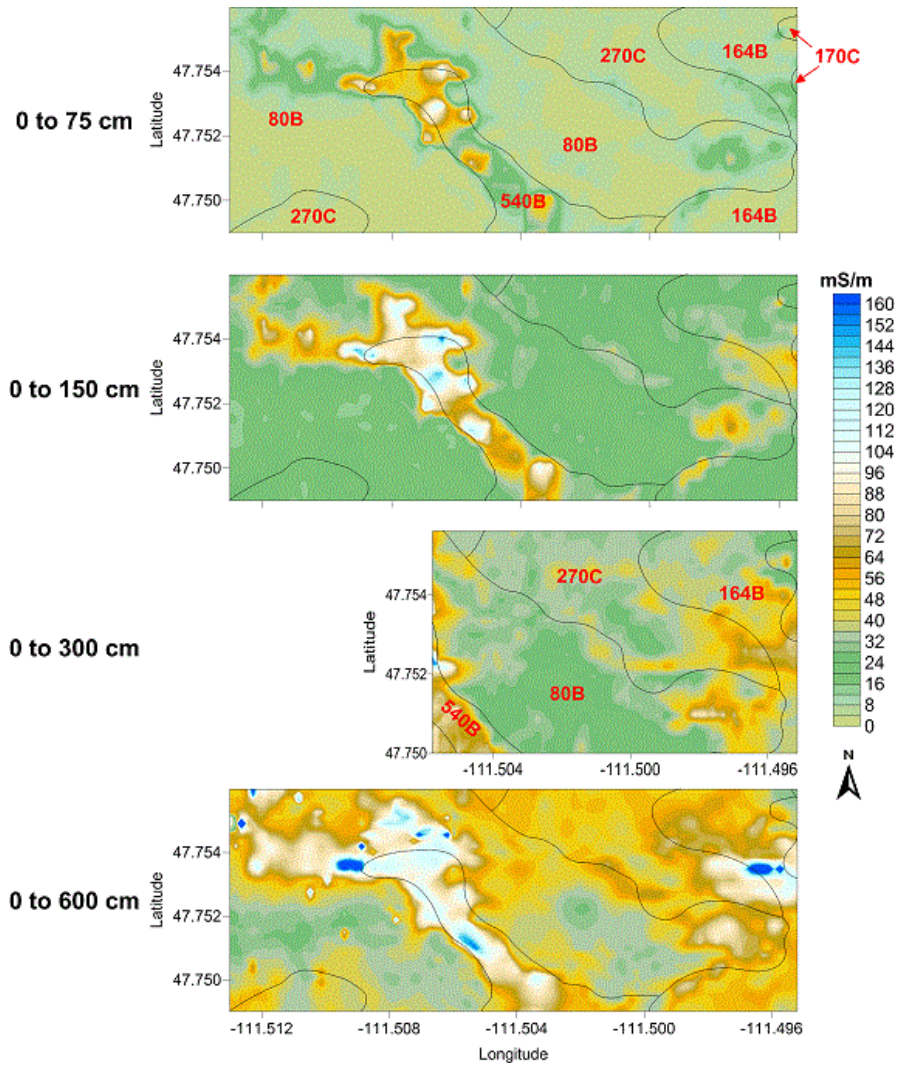


Figure 12. These two-dimensional plots of EC_a were collected with different meters, dipole orientations and intercoil spacings across the Grossman site. Variations in amplitude and spatial patterns are evident for each depth of observation.

Using *EMI indices* (Figure 13), we can see that most of this site is characterized by a normal salt profile (EC_a increases with increasing soil depth; *EMI indices* <1). The *EMI indices* shown in Figure 13 were calculated by dividing the shallower (50 cm intercoil spacing) by the deeper (100 cm intercoil spacing) recordings of the EM38-MK2 meter (upper plot); and by dividing the deeper (100 cm intercoil spacing) recordings of the EM38-MK2 meter by the VDO recordings of the EM31 meter (lower plot). Based on measurements made with the EM38-MK2 meter (upper plot) and for the shallower DOI, all soils within the study site display normal salt profiles. Because of the prevalence of normal salt profiles in the upper plot of Figure 13, it is assumed that salts, if once present in surface layers, have been largely leached to deeper soil depths. Another possible interpretation of this vertical trend is presence of deeper layers with greater clay, moisture and/or soluble salt contents. Only in the lower plot (for the 0 to 6 m depth interval), and along the drainageway is conductivity higher in the surface layers. Here, fragmented areas with either normal or inverted salinity profiles are intermixed. In the lower plot, a northwest to southeast trending lineation to the west of the drainageway in the lower central portion of the site represents a buried utility line.

In both of the plots shown in Figure 13, the more distant the *EMI index* value is from 1, the greater the

contrast in EC_a between the upper and lower depth readings. In the upper plot, noticeable spatial patterns with more extreme *EMI index* values are evident across upland areas and especially in the southern portion of the survey area. Several branching, linear patterns of less extreme *EMI index* values are evident along the lower-lying drainageway and in the eastern (right-hand) portion of the site. For this relatively shallow DOI, these less contrasting *EMI index* values may suggest the likely locations of seepage and more uniform concentration of soluble salts and excess water within the soil profiles. In the lower plot, noticeable patterns of more extreme *EMI index* values are evident along the drainageway composed of Marvan soils.

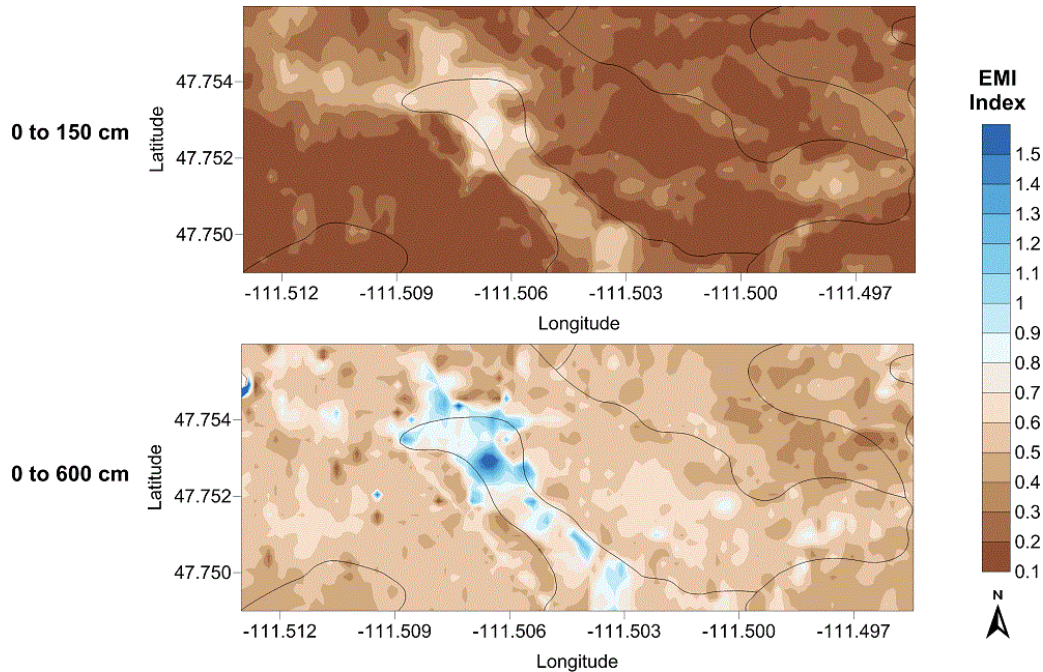


Figure 13. These two-dimensional plots of the Grossman site show the spatial distribution of *EMI indices* for different depths of observation. Soil boundary lines are from the Web Soil Survey.

Figure 14 contains four, 3D wireframe models of the elevation (m) of the Grossman site with superimposed plots of the EC_a data measured with the EM38-MK2 and EM31 meters using different intercoil spacing and/or dipole orientations. The elevation data were obtained during the EMI survey with the Pathfinder ProXT GPS receiver. Soil boundary lines were imported from the Web Soil Survey. The symbols for these map units are shown on the upper plot.

As shown in the 3D simulations of Figure 14, areas with the highest EC_a (suspected saline area) are largely confined to the drainageway and the delineation of Marvan silty clay, wet, 0 to 4 % slopes (540B). On adjoining, more higher-lying and sloping areas of Pylon silty clay loam, 0 to 4 % slopes (80B), EC_a is consistently lower. On each of the plots, an area of relatively higher EC_a is apparent in the extreme eastern (left-hand) portion of the site. This higher-lying portion of the site consists of several different soil map units. Here, the area of higher EC_a becomes more extensive and pronounced with increasing soil depth. Because of the location and vertical distribution of EC_a , seeps are suspected to occur in this area.

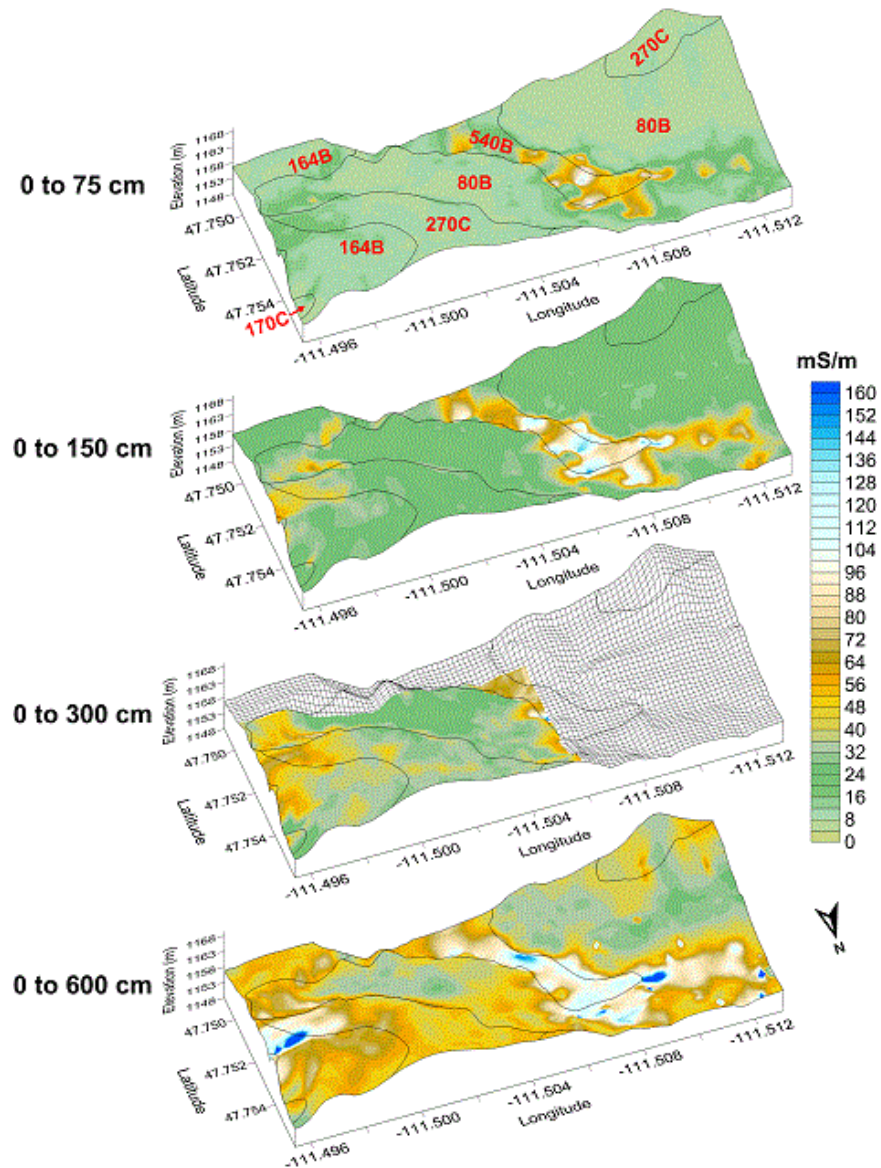


Figure 14. These three-dimensional wireframe images of the elevation at the Grossman site are overlaid by EC_a isoline plots for different depths of observation.

References:

- Black, A.L., P.L. Brown, A.D. Halvorson, and F.H. Siddoway. 1981. Dry land cropping strategies for efficient water-use to control saline seeps in the northern Great Plains, U.S.A. *Agr. Water Manage.* 4:295-311.
- Brown, P.L., A.D. Halvorson, F.H. Siddoway, H.F. Mayland, and M.R. Miller. 1983. Saline-Seep Diagnosis, Control, and Reclamation. U.S. Department of Agriculture Conservation Research Report No. 30, 22p.
- Doering, E.J., and F.M. Sandoval. 1976. Hydrology of saline seeps in the Northern Great Plains. *Trans. ASAE* 19(5): 856-861, 865.

- Geonics Limited, 2009. EM38-MK2-2 ground conductivity meter operating manual. Geonics Ltd., Mississauga, Ontario.
- Halvorson, A.D., 1984. Saline-seep reclamation in the northern Great Plains. *Transactions of the ASAE* 773-778.
- Halvorson, A.D. 1988. Role of cropping systems in environmental quality: Saline seep control. 179-191 pp. *In: Hargrove, W.L. (Ed.). Cropping Strategies for Efficient Use of Water and Nitrogen. ASA Special Publication 51. American Society of Agronomy, Madison, WI*
- Halvorson, A.D. and C.A. Reule. 1980. Alfalfa for hydrologic control of saline seep. *Soil Sci. Soc. Am. J.* 44:370-373.
- Halvorson, A.D., and J.D. Rhoades, 1974. Assessing soil salinity and identifying potential saline-seep areas with field soil resistance measurements. *Soil Science Society of America, Proceedings* 38: 576-581
- Hatton, T., W. Dawes, and P. Richardson, 1994. Can an index based on multi-frequency EMI identify discharge areas? *Australian Journal of Soil and Water Conservation* 7(4): 45-50.
- Lesch, S.M. 2005. Sensor-directed response surface sampling designs for characterizing spatial variation in soil properties. *Computers and Electronic in Agriculture* 46: 153-180.
- Lesch, S.M., J.D. Rhoades and D.L. Corwin. 2000. ESAP-95 version 2.10R User Manual and Tutorial Guide. Research Report 146. USDA-ARS George E. Brown, Jr. Salinity Laboratory, Riverside, California.
- Mankin, K.R., and R. Karthikeyan, 2002. Field assessment of saline seep remediation using electromagnetic induction. *Transaction of ASAE* 45(1): 99-107.
- McNeill, J.D., 1980. Electromagnetic terrain conductivity measurements at low induction numbers. Technical Note TN-6. Geonics Ltd., Mississauga, Ontario.
- Miller, M.R., P.L. Brown, J.J. Donovan, R.N. Bergatino, J.L. Sonderegger, and F.A. Schmidt. 1981. Saline seep development and control in the North American Great Plains – Hydrogeological aspects. *Agr. Water Manage.* 4:115-141.
- Richardson, D.P., and B.G. Williams, 1994. Assessing discharge characteristics of upland landscapes using electromagnetic induction techniques. Technical memorandum 94/3. CSIRO Institute of Natural Resources and Environment, Division of Water Resources. Canberra, Australia.
- Taylor, H.M., 2013. Saline Seep Management in North-central Montana. Unpublished master's thesis Oregon State University, Corvallis, OR
- Williams, B.G., 1983. Electromagnetic induction as an aid to salinity investigations in North East Thailand. Technical Memorandum 83/27. CSIRO Institute of Biological Resources, Division of Water and Land Resources. Canberra, Australia.
- Williams, B.G., and S. Arunin, 1990. Inferring recharge/discharge areas from multifrequency electromagnetic induction measurements. CSIRO Division of Water Resources Tech. Memo. 90/11. CSIRO Institute of Natural Resources and Environment, Division of Water Resources. Canberra, Australia.

Williams, B.G., J. Walker, and J. Anderson, 2006. Spatial variability of regolith leaching and salinity in relation to whole farming planning. *Australian Journal of Experimental Agriculture* 46: 1271-1277.